International Journal of Engineering Sciences & Research Technology

(A Peer Reviewed Online Journal)
Impact Factor: 5.164

IJESRT

RESEARCHERID
THOMSON REUTERS

[Keita *et al.*, 9(8): August, 2020]
IC™ Value: 3.00

ISSN: 2277-9655
Impact Factor: 5.164
CODEN: IJESS7

IJESRT

INTERNATIONAL JOURNAL OF ENGINEERING SCIENCES & RESEARCH TECHNOLOGY

DETERMINATION AND EVOLUTION OF PHOTOELECTRICAL PARAMETERS BASED ON $CUINSE_2$ AND $CUINS_2$ HETEROSTRUCTURE UNDER ILLUMINATION

E.M. Keita*, C. SOW, M.L. Sow, Y. Tabar, C. Sene & B. Mbow
Laboratoire des Semiconducteurs et d'Energie Solaire, Département de Physique, Faculté des Sciences et Techniques, Université Cheikh Anta Diop, Dakar, Sénégal

DOI: https://doi.org/10.29121/ijesrt.v9.i8.2020.7

ABSTRACT

In this paper, we study in the case of monochromatic and polychromatic illuminations, the behavior of the structure ZnO(n+)/CdS(n)/$CuInSe_2$(p)/ $CuInS_2$(p+) where $CuInSe_2$ represent the base and $CuInS_2$ the substrate. ZnO and CdS are used as window layers. We propose the study of the internal quantum efficiency, the generation rate profiles, the photogenerated minority carrier densities and the resulting photocurrent densities, represented versus the junction depth. We consider photon energy ranging between 1.04 eV (λ = 1.192 µm) and 3.1 eV (λ = 0.4 µm). The study of the profiles of these parameters allows to visualize the behavior of the photocreated carriers in the different regions of the structure, to identify the influence of the electrical and geometric parameters on the collection efficiency, shows the transport direction of the carriers and the effects of the interfaces and surfaces on their collection [1].

KEYWORDS: Thin films, $CuInSe_2$, $CuInS_2$, internal quantum efficiency, photoelectrical parameters.

1. INTRODUCTION

$CuInS_2$ and $CuInSe_2$ have similar electrical and lattice parameters but have different energy band gaps. The $CuInSe_2$ has a direct band gap in order to 1.04 eV [2-4] and a lattice matched to the $CuInS_2$ [5-12]. The band gap of the $CuInS_2$ is in the order of 1.57 eV [6]. In this work we propose to study theoretically under polychromatic and monochromatic illuminations the behavior of the heterostructure with increasing energy band gap materials defined by the model ZnO(n+)/CdS(n)/$CuInSe_2$(p)/$CuInS_2$(p+) where the layers ZnO and CdS respectively doped n + and n, are used as large gap window layers. $CuInSe_2$ is used as a base and $CuInS_2$ as a substrate. The substrate doped p+ and the base doped p are the same family (chalcopyrite semiconductor). The p+ doping allows to maintain photocarriers in the base (creating a low potential barrier). It involves studying the intrinsic parameters such as the generation rate, the photogenerated minority carrier densities and the photocurrent densities, which are at the origin of the spectral response. The study of these parameters allows to see and to identify the influence of the electrical and geometrical parameters on the collection efficiency, it shows the transport direction (diffusion) of the carriers and the influence of the interfaces on their collection.

2. MATERIALS AND METHOD

For the structure n^+npp^+, the theoretical model used for the determination of the spectral response and the intrinsic parameters (generation rate, photogenerated minority carrier densities and resulting photocurrent densities) is based on the effects of the absorption coefficients of the different materials and the geometrical and electrical parameters modeling the solar cell (diffusion length, recombination velocity at the front and the back surface and at the interface between different layers, thicknesses of the layers, etc.). It is assumed that the optical reflection coefficient is neglected at each interface in the spectral range used. It is also considered that the space charge region is located only between the p and n regions of each structure and there is no electric field outside this region. Moreover, in this same region, recombination phenomena are neglected.

ISSN: 2277-9655
Impact Factor: 5.164
CODEN: IJESS7

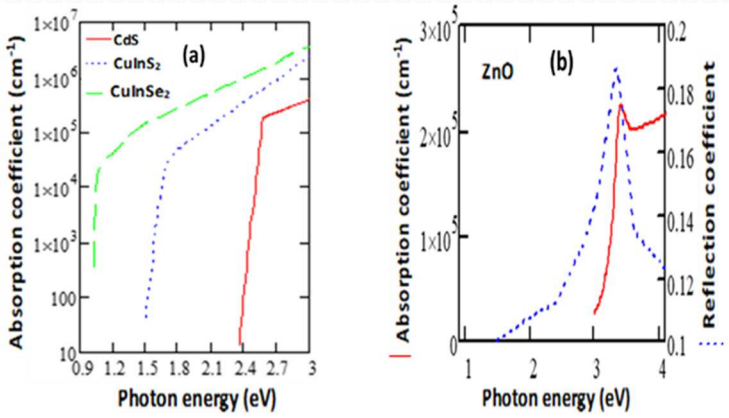

Figure 1. (a) Absorption coefficient of CdS, $CuInS_2$, $CuInSe_2$ materials versus photon energy [1, 5, 6] ; (b) Absorption coefficient and reflection coefficient of ZnO material versus photon energy [13]

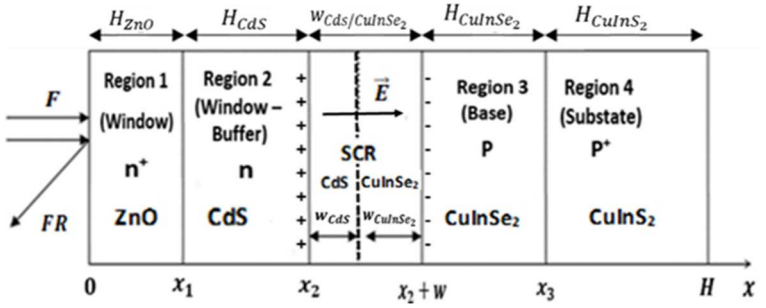

Figure 2 : Diagram of the structure $ZnO(n^+)/CdS(n)CuInSe_2(p)/CuInS_2(p^+)$

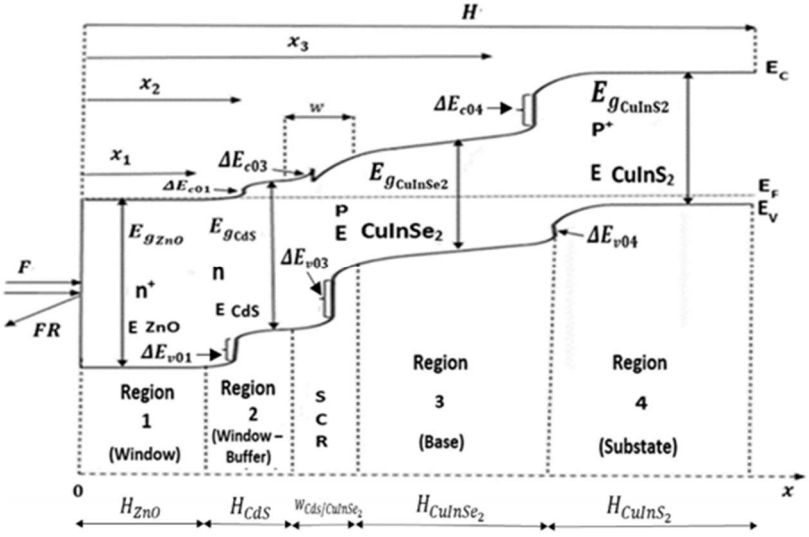

Figure 3 : Energy band diagram of the structure $ZnO(n^+)/CdS(n)CuInSe_2(p)/CuInS_2(p^+)$ [14]

The theoretical study, based on solving a system of differential equations formed by the continuity equations with the optica,l electrical and geometrical parameters of the various materials of the structure, is developed. The solution of these equations depends on the boundary conditions used in the different regions of the structure. However, the literal solution of this problem allows to have precious information for the characterization and the optimization of geometrical and electrical parameters of the different layers by visualizing carrier behaviors in two and three dimensional representation. It also allows to choose the best parameters in order to enhance the

ISSN: 2277-9655
Impact Factor: 5.164
CODEN: IJESS7

solar cell performance. On figures 1 we represent the optical absorption coefficients of the different materials and the ZnO reflection coefficient [1, 5, 6, 13]. The diagram of the structure is shown on figure 2 and the energy band diagram is represented on figure 3 [14].

Calculation of the photocurrent of holes in ZnO layer

In ZnO layer, the photocurrent is essentially due to the holes, the continuity equation is written :

$$\frac{d^2\Delta p_{ZnO}}{dx^2} - \frac{\Delta p_{ZnO}}{{L_{p_{ZnO}}}^2} = \frac{-\alpha_{ZnO}F(1-R_{ZnO})e^{-\alpha_{ZnO}x}}{D_{p_{ZnO}}} \quad (1)$$

With : $${L_{p_{ZnO}}}^2 = D_{p_{ZnO}}\tau_{p_{ZnO}} \quad (2)$$

The expression of the generation rate is given by :

$$G_{ZnO}(x) = \alpha_{ZnO}F(1-R_{ZnO})e^{-\alpha_{ZnO}x} \quad (3)$$

Boundary conditions are given by [1, 5, 15] :

$$D_{p_{ZnO}}\left(\frac{d\Delta p_{ZnO}}{dx}\right) = S_{p_{ZnO}}\Delta p_{ZnO} \quad \text{for} \quad x = 0 \quad (4)$$

$$\Delta p_{ZnO} = 0 \quad \text{for} \quad x = H_{ZnO} \quad (5)$$

The solution of equation (1) gives the expression of the density of holes in ZnO layer, it is written :

$$\Delta p_{ZnO}(x) = -\frac{\alpha_{ZnO}\,{L_{p_{ZnO}}}^2 F(1-R_{ZnO})}{D_{p_{ZnO}}\left(\alpha_{ZnO}{}^2{L_{p_{ZnO}}}^2 - 1\right)} \times \left[e^{-\alpha_{ZnO}\cdot x} + \frac{\left(\frac{S_{p_{ZnO}}L_{p_{ZnO}}}{D_{p_{ZnO}}} + \alpha_{ZnO}L_{p_{ZnO}}\right)\cdot \mathrm{sh}\left(\frac{x-H_{ZnO}}{L_{p_{ZnO}}}\right) - e^{-\alpha_{ZnO}H_{ZnO}}\left[\frac{S_{p_{ZnO}}L_{p_{ZnO}}}{D_{p_{ZnO}}}\cdot \mathrm{sh}\left(\frac{x}{L_{p_{ZnO}}}\right) + \mathrm{ch}\left(\frac{x}{L_{p_{ZnO}}}\right)\right]}{\frac{S_{p_{ZnO}}L_{p_{ZnO}}}{D_{p_{ZnO}}}sh\left(\frac{H_{ZnO}}{L_{p_{ZnO}}}\right) + ch\left(\frac{H_{ZnO}}{L_{p_{ZnO}}}\right)} \right] \quad (6)$$

The expression of the photocurrent density of holes in ZnO layer, is given by :

$$J_{p_{ZnO}}(x) = -qD_{p_{ZnO}}\frac{d\Delta p_{ZnO}}{dx} \quad (7)$$

Calculation of the photocurrent of holes in CdS layer

In CdS layer, the photocurrent is also a hole current. The interface effects are characterized by a recombination velocity at the interface ZnO/CdS noted $S_{p_{ZnO/CdS}}$. The continuity equation is given by :

$$\frac{d^2\Delta p_{CdS}}{dx^2} - \frac{\Delta p_{CdS}}{{L_{p_{CdS}}}^2} = \frac{-\alpha_{CdS}F(1-R_{ZnO})e^{-\alpha_{ZnO}H_{ZnO}}e^{-\alpha_{CdS}(x-H_{ZnO})}}{D_{p_{CdS}}} \quad (8)$$

With : $${L_{p_{CdS}}}^2 = D_{p_{CdS}}\tau_{p_{CdS}} \quad (9)$$

The expression of the generation rate is given by :

$$G_{CdS}(x) = \alpha_{CdS}F(1-R_{ZnO})e^{-\alpha_{ZnO}H_{ZnO}}e^{-\alpha_{CdS}(x-H_{ZnO})} \quad (10)$$

Boundary conditions are given by [1, 5, 16, 17] :

$$D_{p_{CdS}}\frac{d\Delta p_{CdS}}{dx} = S_{p_{ZnO/CdS}}\Delta p_{CdS} + D_{p_{ZnO}}\frac{d\Delta p_{ZnO}}{dx} \quad \text{for } x = H_{ZnO} \quad (11)$$

$$\Delta p_{CdS} = 0 \quad \text{for } x = H_{CdS} + H_{ZnO} \quad (12)$$

The solution of equation (8) gives the density of holes in CdS layer, it is given by :

$$\Delta p_{CdS}(x) = \Delta p_2(x) + \Delta p_1(x) \quad (13)$$

$$\Delta p_2(x) = -\frac{\alpha_{CdS}\,{L_{p_{CdS}}}^2 F(1-R_{ZnO})\,e^{-\alpha_{ZnO}H_{ZnO}}}{D_{p_{CdS}}\left(\alpha_{CdS}{}^2{L_{p_{CdS}}}^2 - 1\right)}\cdot \left[e^{-\alpha_{CdS}(x-H_{ZnO})} + \frac{\left(\frac{S_{p_{ZnO/CdS}}L_{p_{CdS}}}{D_{p_{CdS}}} + \alpha_{CdS}L_{p_{CdS}}\right)\cdot \mathrm{sh}\left(\frac{x-(H_{ZnO}+H_{CdS})}{L_{p_{CdS}}}\right) - e^{-\alpha_{CdS}H_{CdS}}\left[\frac{S_{p_{ZnO/CdS}}L_{p_{CdS}}}{D_{p_{CdS}}}\cdot \mathrm{sh}\left(\frac{x-H_{ZnO}}{L_{p_{CdS}}}\right) + \mathrm{ch}\left(\frac{x-H_{ZnO}}{L_{p_{CdS}}}\right)\right]}{\frac{S_{p_{ZnO/CdS}}L_{p_{CdS}}}{D_{p_{CdS}}}sh\left(\frac{H_{CdS}}{L_{p_{CdS}}}\right) + ch\left(\frac{H_{CdS}}{L_{p_{CdS}}}\right)} \right] \quad (13\text{-a})$$

$$\Delta p_1(x) = -\frac{\mathrm{sh}\left(\frac{x-(H_{ZnO}+H_{CdS})}{L_{p_{CdS}}}\right)\cdot \alpha_{ZnO}\,F(1-R_{ZnO})\,L_{p_{ZnO}}L_{p_{CdS}}}{D_{p_{CdS}}\left(\alpha_{ZnO}{}^2{L_{p_{ZnO}}}^2 - 1\right)\left\{\frac{S_{p_{ZnO/CdS}}L_{p_{CdS}}}{D_{p_{CdS}}}sh\left(\frac{H_{CdS}}{L_{p_{CdS}}}\right) + ch\left(\frac{H_{CdS}}{L_{p_{CdS}}}\right)\right\}} \times \left\{ \frac{\left(\frac{S_{p_{ZnO}}L_{p_{ZnO}}}{D_{p_{ZnO}}} + \alpha_{ZnO}L_{p_{ZnO}}\right) - e^{-\alpha_{ZnO}H_{ZnO}}\left[\frac{S_{p_{ZnO}}L_{p_{ZnO}}}{D_{p_{ZnO}}}ch\left(\frac{H_{ZnO}}{L_{p_{ZnO}}}\right) + sh\left(\frac{H_{ZnO}}{L_{p_{ZnO}}}\right)\right]}{\frac{S_{p_{ZnO}}L_{p_{ZnO}}}{D_{p_{ZnO}}}sh\left(\frac{H_{ZnO}}{L_{p_{ZnO}}}\right) + ch\left(\frac{H_{ZnO}}{L_{p_{ZnO}}}\right)} - \alpha_{ZnO}L_{p_{ZnO}}e^{-\alpha_{ZnO}H_{ZnO}} \right\} \quad (13\text{-b})$$

The expression of the resulting photocurrent density of holes in CdS layer is given by :

ISSN: 2277-9655
Impact Factor: 5.164
CODEN: IJESS7

$$J_{pcds}(x) = -qD_{pcds}\frac{d\Delta p_{cds}}{dx} \quad (14)$$

Calculation of the photocurrent in the space charge region

In the space charge region, the recombinations of carriers are neglected. It is formed by two areas : the first area is formed by CdS layer, the thickness is fixed at w_{CdS}, the continuity equation for the photo-created holes is written as :

$$-\frac{1}{q}\frac{dJ_{wCdS}}{dx} + \alpha_{cds}F(1-R_{ZnO})\ e^{-\alpha_{ZnO}H_{ZnO}}e^{-\alpha_{cds}(x-H_{ZnO})} = 0 \quad (15)$$

With : $$J_{wCdS}(x) = 0 \qquad \text{for } x = H_{CdS} + H_{ZnO} \quad (16)$$

The photocurrent density of holes in this first area (CdS), is given by the solution of equation (15), it is written as :

$$J_{wCdS}(x) = -qF(1-R_{ZnO})e^{-\alpha_{ZnO}H_{ZnO}}\left[e^{-\alpha_{cds}(x-H_{ZnO})} - e^{-\alpha_{cds}H_{cds}}\right] \quad (17)$$

The second area is formed by $CuInSe_2$ layer, the thickness is fixed at $w_{CuInSe2}$, the continuity equation for the photo-created holes is written as :

$$-\frac{1}{q}\frac{dJ_{w_{CuInSe_2}}}{dx} + \alpha_{CuInSe_2}F(1-R_{ZnO})e^{-\alpha_{ZnO}H_{ZnO}}e^{-\alpha_{cds}(H_{cds}+w_{cds})}e^{-\alpha_{CuInSe_2}[x-(H_{ZnO}+H_{cds}+w_{cds})]} = 0 \quad (18)$$

With : $$J_{w_{CuInSe_2}}(x) = 0 \qquad \text{for } x = H_{ZnO} + H_{CdS} + w_{CdS} \quad (19)$$

The photocurrent density of holes in this second area ($CuInSe_2$), is given by the solution of equation (18), it is written as :

$$J_{w_{CuInSe_2}}(x) = -qF(1-R_{ZnO})e^{-\alpha_{ZnO}H_{ZnO}}e^{-\alpha_{cds}(H_{cds}+w_{cds})}\left[e^{-\alpha_{CuInSe_2}[x-(H_{ZnO}+H_{cds}+w_{cds})]} - 1\right] \quad (20)$$

Calculation of the photocurrent in $CuInS_2$ layer

In $CuInS_2$ layer, the photocurrent is due to the photo-created electrons, the continuity equation is given by :

$$\frac{d^2\Delta n_{CuInS_2}}{dx^2} - \frac{\Delta n_{CuInS_2}}{L^2_{n_{CuInS_2}}} = \frac{-\alpha_{CuInS_2}}{D_{n_{CuInS_2}}}F(1-R_{ZnO})e^{-\alpha_{ZnO}H_{ZnO}} \times e^{-\alpha_{cds}(H_{cds}+w_{cds})}e^{-\alpha_{CuInSe_2}\left(H_{CuInSe_2}+w_{CuInSe_2}\right)} \times e^{-\alpha_{CuInS_2}\left[x-\left(H-H_{CuInS_2}\right)\right]} \quad (21)$$

The expression of the generation rate is given by :

$$G_{CuInS_2}(x) = \alpha_{CuInS_2}F(1-R_{ZnO})e^{-\alpha_{ZnO}H_{ZnO}} \times e^{-\alpha_{cds}(H_{cds}+w_{cds})}e^{-\alpha_{CuInSe_2}\left(H_{CuInSe_2}+w_{CuInSe_2}\right)} \times e^{-\alpha_{CuInS_2}\left[x-\left(H-H_{CuInS_2}\right)\right]} \quad (22)$$

Boundary conditions are given by [1, 5, 15] :

$$D_{n_{CuInS_2}}\frac{d\Delta n_{CuInS_2}}{dx} = -S_{n_{CuInS_2}}\Delta n_{CuInS_2} \quad \text{for } x = H \quad (23)$$

$$\Delta n_{CuInS_2} = 0 \quad \text{for} \quad x = H - H_{\text{CuInS2}} \quad (24)$$

The density of photo-created electrons in $CuInS_2$ is solution of equation (21), It is given by :

$$\Delta n_{CuInS_2}(x) = -\frac{\alpha_{CuInS_2}L_{n_{CuInS_2}}{}^2F(1-R_{ZnO})\,e^{\left[(\alpha_{cds}-\alpha_{ZnO})H_{ZnO}\right]}e^{\left[(\alpha_{CuInSe_2}-\alpha_{cds})(H_{ZnO}+H_{cds}+w_{cds})\right]}e^{\left[(\alpha_{CuInS_2}-\alpha_{CuInSe_2})(H-H_{CuInS_2})\right]}}{D_{n_{CuInS_2}}\left(\alpha_{CuInS_2}{}^2L_{n_{CuInS_2}}{}^2-1\right)} \times \left[e^{-\alpha_{CuInS_2}x} + \frac{\left(\alpha_{CuInS_2}L_{n_{CuInS_2}} - \frac{S_{n_{CuInS_2}}L_{n_{CuInS_2}}}{D_{n_{CuInS_2}}}\right)e^{-\alpha_{CuInS_2}H}\cdot\mathrm{sh}\left(\frac{x-\left(H-H_{CuInS_2}\right)}{L_{n_{CuInS_2}}}\right)}{\frac{S_{n_{CuInS_2}}L_{n_{CuInS_2}}}{D_{n_{CuInS_2}}}sh\left(\frac{H_{CuInS_2}}{L_{n_{CuInS_2}}}\right)+ch\left(\frac{H_{CuInS_2}}{L_{n_{CuInS_2}}}\right)} - \frac{e^{-\alpha_{CuInS_2}\left(H-H_{CuInS_2}\right)}\left[\frac{S_{n_{CuInS_2}}L_{n_{CuInS_2}}}{D_{n_{CuInS_2}}}\cdot\mathrm{sh}\left(\frac{H-x}{L_{n_{CuInS_2}}}\right)+\mathrm{ch}\left(\frac{H-x}{L_{n_{CuInS_2}}}\right)\right]}{\frac{S_{n_{CuInS_2}}L_{n_{CuInS_2}}}{D_{n_{CuInS_2}}}sh\left(\frac{H_{CuInS_2}}{L_{n_{CuInS_2}}}\right)+ch\left(\frac{H_{CuInS_2}}{L_{n_{CuInS_2}}}\right)}\right] \quad (25)$$

The resulting photocurrent density of electrons in $CuInS_2$ layer is given by :

$$J_{n_{CuInS_2}}(x) = qD_{n_{CuInS_2}}\frac{d\Delta n_{CuInS_2}}{dx} \quad (26)$$

Calculation of the photocurrent in $CuInSe_2$ layer

In $CuInSe_2$ layer, the photocurrent is also due to the photo-created electrons, the continuity equation is given by :

$$\frac{d^2\Delta n_{CuInSe_2}}{dx^2} - \frac{\Delta n_{CuInSe_2}}{L^2_{CuInSe_2}} = \frac{-\alpha_{CuInSe_2}}{D_{n_{CuInSe_2}}}F(1-R_{ZnO})e^{-\alpha_{ZnO}H_{ZnO}}e^{-\alpha_{cds}(H_{cds}+w_{cds})}e^{-\alpha_{CuInSe_2}[x-(H_{ZnO}+H_{cds}+w_{cds})]} \quad (27)$$

The expression of the generation rate is given by :

ISSN: 2277-9655
Impact Factor: 5.164
CODEN: IJESS7

$$G_{CuInSe_2}(x) = \alpha_{CuInSe_2} F(1-R_{ZnO}) e^{-\alpha_{ZnO} H_{ZnO}} e^{-\alpha_{CdS}(H_{CdS}+w_{CdS})} e^{-\alpha_{CuInSe_2}[x-(H_{ZnO}+H_{CdS}+w_{CdS})]} \quad (28)$$

The interface effects are characterized by a recombination velocity at the interface $CuInSe_2/CuInS_2$ noted $S_{n_{CuInSe_2/CuInS_2}}$.

Boundary conditions can be written as [14] :

$$\Delta n_{CuInSe_2} = 0 \quad \text{for} \quad x = H_{ZnO} + H_{CdS} + w_{CdS} + w_{\text{CuInSe2}} \quad (29)$$

$$D_{n_{CuInSe_2}} \frac{d\Delta n_{CuInSe_2}}{dx} = -S_{n_{CuInSe_2/CuInS_2}} \Delta n_{CuInSe_2} + D_{n_{CuInS_2}} \frac{d\Delta n_{CuInS_2}}{dx} \quad \text{for } x = H - H_{\text{CuInS2}} \quad (30)$$

The density of photo-created electrons in $CuInSe_2$ layer, is solution of equation (27), It is given by :

$$\Delta n_{CuInSe_2}(x) = \Delta n_3(x) + \Delta n_4(x) \quad (31)$$

$$\Delta n_3(x) = -\frac{\alpha_{CuInSe_2} {L_n}_{CuInSe_2}{}^2 F(1-R_{ZnO})\, e^{[(\alpha_{CdS}-\alpha_{ZnO})H_{ZnO}]}\, e^{\left[(\alpha_{CuInSe_2}-\alpha_{CdS})(H_{ZnO}+H_{CdS}+w_{CdS})\right]}}{D_{n_{CuInSe_2}}\left(\alpha_{CuInSe_2}{}^2 {L_n}_{CuInSe_2}{}^2 - 1\right)} \times \left[e^{-\alpha_{CuInSe_2} x} + \right.$$

$$\frac{\left(\alpha_{CuInSe_2} L_{n_{CuInSe_2}} - \frac{S_{n_{CuInSe_2/CuInS_2}} {L_n}_{CuInSe_2}}{D_{n_{CuInSe_2}}}\right) e^{-\alpha_{CuInSe_2}\left(H-H_{CuInS_2}\right)} \cdot \mathrm{sh}\left[\frac{x-\left(H_{ZnO}+H_{CdS}+w_{CdS}+w_{CuInSe_2}\right)}{L_{n_{CuInSe_2}}}\right]}{\frac{S_{n_{CuInSe_2/CuInS_2}} {L_n}_{CuInSe_2}}{D_{n_{CuInSe_2}}} \mathrm{sh}\left[\frac{H_{CuInSe_2}}{L_{n_{CuInSe_2}}}\right] + \mathrm{ch}\left[\frac{H_{CuInSe_2}}{L_{n_{CuInSe_2}}}\right]} -$$

$$\left. \frac{e^{-\alpha_{CuInSe_2}\left(H_{ZnO}+H_{CdS}+w_{CdS}+w_{CuInSe_2}\right)} \left[\frac{S_{n_{CuInSe_2/CuInS_2}} {L_n}_{CuInSe_2}}{D_{n_{CuInSe_2}}} \mathrm{sh}\left(\frac{\left(H-H_{CuInS_2}\right)-x}{L_{n_{CuInSe_2}}}\right) + \mathrm{ch}\left(\frac{\left(H-H_{CuInS_2}\right)-x}{L_{n_{CuInSe_2}}}\right)\right]}{\frac{S_{n_{CuInSe_2/CuInS_2}} {L_n}_{CuInSe_2}}{D_{n_{CuInSe_2}}} \mathrm{sh}\left[\frac{H_{CuInSe_2}}{L_{n_{CuInSe_2}}}\right] + \mathrm{ch}\left[\frac{H_{CuInSe_2}}{L_{n_{CuInSe_2}}}\right]} \right] \quad (31\text{-a})$$

$$\Delta n_4(x) =$$

$$-\frac{\mathrm{sh}\left[\frac{x-\left(H_{ZnO}+H_{CdS}+w_{CdS}+w_{CuInSe_2}\right)}{L_{n_{CuInSe_2}}}\right] \alpha_{CuInS_2} {L_n}_{CuInS_2} {L_n}_{CuInSe_2} F(1-R_{ZnO})\, e^{[(\alpha_{CdS}-\alpha_{ZnO})H_{ZnO}]}\, e^{\left[(\alpha_{CuInSe_2}-\alpha_{CdS})(H_{ZnO}+H_{CdS}+w_{CdS})\right]}}{D_{n_{CuInSe_2}}\left(\alpha_{CuInS_2}{}^2 {L_n}_{CuInS_2}{}^2 - 1\right)\left\{\frac{S_{n_{CuInSe_2/CuInS_2}} {L_n}_{CuInSe_2}}{D_{n_{CuInSe_2}}} \mathrm{sh}\left[\frac{H_{CuInSe_2}}{L_{n_{CuInSe_2}}}\right] + \mathrm{ch}\left[\frac{H_{CuInSe_2}}{L_{n_{CuInSe_2}}}\right]\right\}} \times$$

$$e^{\left[(\alpha_{CuInS_2}-\alpha_{CuInSe_2})(H-H_{CuInS_2})\right]} \times \left[\frac{\left(\alpha_{CuInS_2} L_{n_{CuInS_2}} - \frac{S_{n_{CuInS_2}} {L_n}_{CuInS_2}}{D_{n_{CuInS_2}}}\right) e^{-\alpha_{CuInS_2} H}}{\frac{S_{n_{CuInS_2}} {L_n}_{CuInS_2}}{D_{n_{CuInS_2}}} \mathrm{sh}\left(\frac{H_{CuInS_2}}{L_{n_{CuInS_2}}}\right) + \mathrm{ch}\left(\frac{H_{CuInS_2}}{L_{n_{CuInS_2}}}\right)} + \right.$$

$$\left. \frac{e^{-\alpha_{CuInS_2}\left(H-H_{CuInS_2}\right)} \left[\frac{S_{n_{CuInS_2}} {L_n}_{CuInS_2}}{D_{n_{CuInS_2}}} \mathrm{ch}\left(\frac{H_{CuInS_2}}{L_{n_{CuInS_2}}}\right) + \mathrm{sh}\left(\frac{H_{CuInS_2}}{L_{n_{CuInS_2}}}\right)\right]}{\frac{S_{n_{CuInS_2}} {L_n}_{CuInS_2}}{D_{n_{CuInS_2}}} \mathrm{sh}\left(\frac{H_{CuInS_2}}{L_{n_{CuInS_2}}}\right) + \mathrm{ch}\left(\frac{H_{CuInS_2}}{L_{n_{CuInS_2}}}\right)} - \alpha_{CuInS_2} L_{n_{CuInS_2}} e^{-\alpha_{CuInS_2}\left(H-H_{CuInS_2}\right)} \right] \quad (31\text{-b})$$

The expression of the photocurrent density of electrons in $CuInSe_2$ layer is given by :

$$J_{n_{CuInSe_2}}(\mathrm{x}) = qD_{n_{CuInSe_2}} \frac{d\Delta n_{CuInSe_2}}{dx} \quad (32)$$

Calculation of the total photocurrent

Carriers which reach the space charge region are assumed to be collected. The total photocurrent collected is the sum of the photocurrents of the different layers, that pass through the space charge region, it is given by the following equation :

$$J_{ph} = J_{ZnO-CdS} + J_{w_{CdS}} + J_{w_{CuInSe_2}} + J_{CuInSe_2-CuInS_2} \quad (33)$$

By noting : $J_{ZnO-CdS} = -qD_{p_{CdS}} \left.\frac{d\Delta p_{CdS}}{dx}\right|_{x=H_{CdS}+H_{ZnO}}$; $J_{w_{CdS}} = J_{w_{CdS}}(H_{ZnO}+H_{CdS}+w_{CdS})$; $J_{w_{CuInSe_2}} = J_{w_{CuInSe_2}}(H_{ZnO}+H_{CdS}+w_{CdS}+w_{\text{CuInSe2}})$; $J_{CuInSe_2-CuInS_2} = qD_{n_{CuInSe_2}} \left.\frac{d\Delta n_{CuInSe_2}}{dx}\right|_{x=H_{ZnO}+H_{CdS}+w_{CdS}+w_{\text{CuInSe2}}}$

We obtain :

ISSN: 2277-9655
Impact Factor: 5.164
CODEN: IJESS7

$$J_{ZnO-CdS} = \frac{q\alpha_{CdS}\,F(1-R_{ZnO})\,L_{p_{CdS}}e^{-\alpha_{ZnO}\,H_{ZnO}}}{\left(\alpha_{CdS}{}^2L_{p_{CdS}}{}^2-1\right)} \times \left\{ \frac{\left(\frac{S_{p_{ZnO/CdS}}L_{p_{CdS}}}{D_{p_{CdS}}}+\alpha_{CdS}\,L_{p_{CdS}}\right)}{\frac{S_{p_{ZnO/CdS}}L_{p_{CdS}}}{D_{p_{CdS}}}sh\left(\frac{H_{CdS}}{L_{p_{CdS}}}\right)+ch\left(\frac{H_{CdS}}{L_{p_{CdS}}}\right)} - \frac{e^{-\alpha_{CdS}\,H_{CdS}}\left[\frac{S_{p_{ZnO/CdS}}L_{p_{CdS}}}{D_{p_{CdS}}}ch\left(\frac{H_{CdS}}{L_{p_{CdS}}}\right)+sh\left(\frac{H_{CdS}}{L_{p_{CdS}}}\right)\right]}{\frac{S_{p_{ZnO/CdS}}L_{p_{CdS}}}{D_{p_{CdS}}}sh\left(\frac{H_{CdS}}{L_{p_{CdS}}}\right)+ch\left(\frac{H_{CdS}}{L_{p_{CdS}}}\right)} - \alpha_{CdS}L_{p_{CdS}}e^{-\alpha_{CdS}H_{CdS}} \right\} +$$

$$\frac{q\alpha_{ZnO}\,F(1-R_{ZnO})\,L_{p_{ZnO}}}{\left(\alpha_{ZnO}{}^2L_{p_{ZnO}}{}^2-1\right)\left[\frac{S_{p_{ZnO/CdS}}L_{p_{CdS}}}{D_{p_{CdS}}}sh\left(\frac{H_{CdS}}{L_{p_{CdS}}}\right)+ch\left(\frac{H_{CdS}}{L_{p_{CdS}}}\right)\right]} \times \left\{ \frac{\left(\frac{S_{p_{ZnO}}L_{p_{ZnO}}}{D_{p_{ZnO}}}+\alpha_{ZnO}L_{p_{ZnO}}\right)}{\frac{S_{p_{ZnO}}L_{p_{ZnO}}}{D_{p_{ZnO}}}sh\left(\frac{H_{ZnO}}{L_{p_{ZnO}}}\right)+ch\left(\frac{H_{ZnO}}{L_{p_{ZnO}}}\right)} - \frac{e^{-\alpha_{ZnO}\,H_{ZnO}}\left[\frac{S_{p_{ZnO}}L_{p_{ZnO}}}{D_{p_{ZnO}}}ch\left(\frac{H_{ZnO}}{L_{p_{ZnO}}}\right)+sh\left(\frac{H_{ZnO}}{L_{p_{ZnO}}}\right)\right]}{\frac{S_{p_{ZnO}}L_{p_{ZnO}}}{D_{p_{ZnO}}}sh\left(\frac{H_{ZnO}}{L_{p_{ZnO}}}\right)+ch\left(\frac{H_{ZnO}}{L_{p_{ZnO}}}\right)} - \alpha_{ZnO}L_{p_{ZnO}}e^{-\alpha_{ZnO}\,H_{ZnO}} \right\} \quad (34)$$

$$J_{w_{CdS}} = -qF(1-R_{ZnO})e^{-\alpha_{ZnO}\,H_{ZnO}}\;e^{-\alpha_{CdS}\,H_{CdS}} \times \left[e^{-\alpha_{CdS}\,w_{CdS}}-1\right] \quad (35)$$

$$J_{w_{CuInSe_2}} = -qF(1-R_{ZnO})e^{-\alpha_{ZnO}\,H_{ZnO}}e^{-\alpha_{CdS}(H_{CdS}+w_{CdS})} \times \left[e^{-\alpha_{CuInSe_2}w_{CuInSe_2}}-1\right] \quad (36)$$

$$J_{CuInSe_2-CuInS_2} = J_3 + J_4 \quad (37$$

$$J_3 == -\frac{q\;\alpha_{CuInSe_2}\,L_{n_{CuInSe_2}}F(1-R_{ZnO})\,e^{\left[(\alpha_{CdS}-\alpha_{ZnO})H_{ZnO}\right]}\,e^{\left[(\alpha_{CuInSe_2}-\alpha_{CdS})(H_{ZnO}+H_{CdS}+w_{CdS})\right]}}{\left(\alpha_{CuInSe_2}{}^2L_{n_{CuInSe_2}}{}^2-1\right)} \times$$

$$\left[\frac{\left(\alpha_{CuInSe_2}L_{n_{CuInSe_2}}-\frac{S_{n_{CuInSe_2/CuInS_2}}L_{n_{CuInSe_2}}}{D_{n_{CuInSe_2}}}\right)e^{-\alpha_{CuInSe_2}\left(H-H_{CuInS_2}\right)}}{\frac{S_{n_{CuInSe_2/CuInS_2}}L_{n_{CuInSe_2}}}{D_{n_{CuInSe_2}}}sh\left[\frac{H_{CuInSe_2}}{L_{n_{CuInSe_2}}}\right]+ch\left[\frac{H_{CuInSe_2}}{L_{n_{CuInSe_2}}}\right]} + \frac{e^{-\alpha_{CuInSe_2}\left(H_{ZnO}+H_{CdS}+w_{CdS}+w_{CuInSe_2}\right)}\left[\frac{S_{n_{CuInSe_2/CuInS_2}}L_{n_{CuInSe_2}}}{D_{n_{CuInSe_2}}}\mathrm{ch}\left(\frac{H_{CuInSe_2}}{L_{n_{CuInSe_2}}}\right)+\mathrm{sh}\left(\frac{H_{CuInSe_2}}{L_{n_{CuInSe_2}}}\right)\right]}{\frac{S_{n_{CuInSe_2/CuInS_2}}L_{n_{CuInSe_2}}}{D_{n_{CuInSe_2}}}sh\left[\frac{H_{CuInSe_2}}{L_{n_{CuInSe_2}}}\right]+ch\left[\frac{H_{CuInSe_2}}{L_{n_{CuInSe_2}}}\right]} - \right.$$

$$\left.\alpha_{CuInSe_2}L_{n_{CuInSe_2}}e^{-\alpha_{CuInSe_2}\left(H_{ZnO}+H_{CdS}+w_{CdS}+w_{CuInSe_2}\right)}\right] \quad (37\text{-a})$$

$$J_4 =$$

$$-\frac{q\;\alpha_{CuInS_2}L_{n_{CuInS_2}}F(1-R_{ZnO})\,e^{\left[(\alpha_{CdS}-\alpha_{ZnO})H_{ZnO}\right]}\,e^{\left[(\alpha_{CuInSe_2}-\alpha_{CdS})(H_{ZnO}+H_{CdS}+w_{CdS})\right]}e^{\left[(\alpha_{CuInS_2}-\alpha_{CuInSe_2})(H-H_{CuInS_2})\right]}}{\left(\alpha_{CuInS_2}{}^2L_{n_{CuInS_2}}{}^2-1\right)\left\{\frac{S_{n_{CuInSe_2/CuInS_2}}L_{n_{CuInSe_2}}}{D_{n_{CuInSe_2}}}sh\left[\frac{H_{CuInSe_2}}{L_{n_{CuInSe_2}}}\right]+ch\left[\frac{H_{CuInSe_2}}{L_{n_{CuInSe_2}}}\right]\right\}} \times$$

$$\left[\frac{\left(\alpha_{CuInS_2}L_{n_{CuInS_2}}-\frac{S_{n_{CuInS_2}}L_{n_{CuInS_2}}}{D_{n_{CuInS_2}}}\right)e^{-\alpha_{CuInS_2}\,H}}{\frac{S_{n_{CuInS_2}}L_{n_{CuInS_2}}}{D_{n_{CuInS_2}}}sh\left(\frac{H_{CuInS_2}}{L_{n_{CuInS_2}}}\right)+ch\left(\frac{H_{CuInS_2}}{L_{n_{CuInS_2}}}\right)} + \frac{e^{-\alpha_{CuInS_2}\left(H-H_{CuInS_2}\right)}\left[\frac{S_{n_{CuInS_2}}L_{n_{CuInS_2}}}{D_{n_{CuInS_2}}}\mathrm{ch}\left(\frac{H_{CuInS_2}}{L_{n_{CuInS_2}}}\right)+\mathrm{sh}\left(\frac{H_{CuInS_2}}{L_{n_{CuInS_2}}}\right)\right]}{\frac{S_{n_{CuInS_2}}L_{n_{CuInS_2}}}{D_{n_{CuInS_2}}}sh\left(\frac{H_{CuInS_2}}{L_{n_{CuInS_2}}}\right)+ch\left(\frac{H_{CuInS_2}}{L_{n_{CuInS_2}}}\right)} - \right.$$

$$\left.\alpha_{CuInS_2}L_{n_{CuInS_2}}e^{-\alpha_{CuInS_2}\left(H-H_{CuInS_2}\right)}\right] \quad (37\text{-b})$$

The internal quantum efficiency (or spectral response) IQE is given by [1, 5, 18] :

$$\mathrm{IQE} = \frac{J_{ZnO-CdS}+J_{w_{CdS}}+J_{w_{CuInSe_2}}+J_{CuInSe_2-CuInS_2}}{qF(1-R)} \quad (38)$$

ISSN: 2277-9655
Impact Factor: 5.164
CODEN: IJESS7

3. RESULTS AND DISCUSSION

Behavior of the structure under monochromatic illumination

In this part, we particularly study the profiles of the generation rate, the minority carrier densities and photocurrent densities versus the depth of the junction, under monochromatic illumination. We consider radiation energies ranging between 1.04 eV (λ = 1.192 µm) and 3.1 eV (λ = 0.4 µm). We consider the parameters of table 1.

Table 1 : physical parameters considered

Layer (Region i)	Thicknes H_i (µm)	diffusion length L_{p_i}, L_{n_i} (µm)	recombination velocity S_{p_i}, S_{n_i} $(cm.s^{-1})$	Mobility coefficient μ_{p_i}, μ_{n_i} $(cm^2/V.s)$	Diffusion coefficient D_{p_i}, D_{n_i} $(cm^2.s^{-1})$
ZnO (n^+) (Region 1)	0.3	0.3	2×10^7	20	0.51
CdS (n) (Region 2)	0.1	0.4	2×10^4	25	0.64
$CuInSe_2$ (p) (Region 3: Base)	1	3	2×10^3	400	10.27
$CuInS_2$ (p^+) (Region 4: Substrate)	98.5	1	2×10^7	200	5.13

$w_1 = 0.02\mu m$; $w_2 = 0.08\mu m$; $H = 100\mu m$

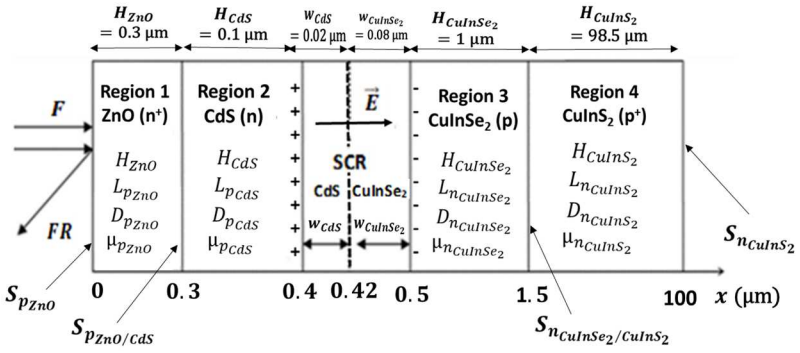

Figure 4 : diagram of the structure and the geometrical parameters

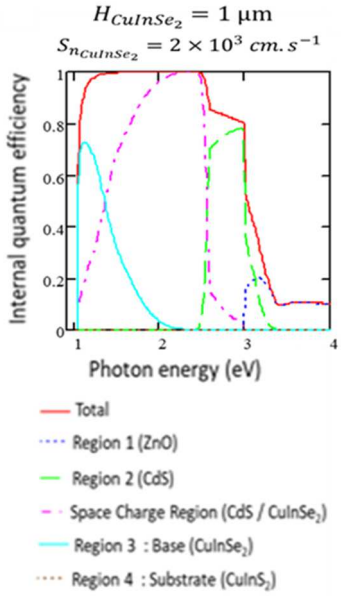

Figure 5. Internal quantum efficiency vs. photon energy

Figure 5 shows for the considered parameters, the global internal efficiency (red curve) versus photon energy and the contribution of the different regions of the structure to the efficiency. We note substrate contribution ($CuInS_2$) does not appear on the graph and a high contribution of the space charge region to the spectral response compared to the other regions. We also note the absorption of the frontal regions (CdS and ZnO) causes a decrease of the global efficiency.

Generation rate profile

On Figures 6-a ad 6-b, we represent the generation rate profiles versus the thickness of the structure for different radiation energies. On Figure 6-b, the peak observed between x = 0.3 µm and x = 0.4 µm for E = 3.1 eV (λ = 0.4

ISSN: 2277-9655
Impact Factor: 5.164
CODEN: IJESS7

µm) corresponds to the absorption of photons by the CdS layer (peak G_{CdS}). On Figures 6-a and 6-b, the peaks obtained between x = 0.4 µm and x = 0.6 µm for photon energy ranging between 1.55 eV and 2.54 eV correspond to absorption of photons by $CuInSe_2$ layer (peak G_{CuInSe_2}).

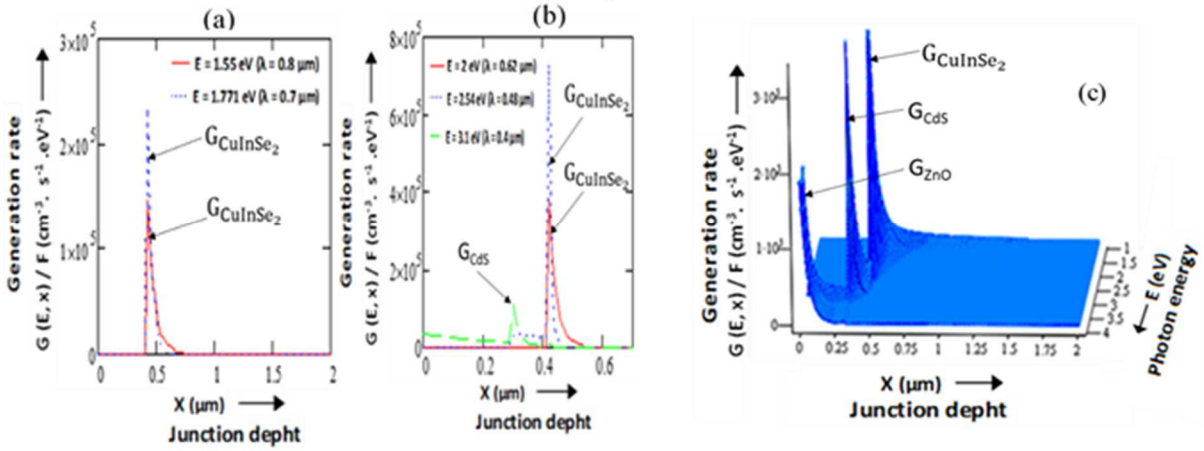

Figure 6. (a) and (b) Generation rate vs. junction depth (x) under monochromatic illumination, (c) Three-dimensional representation of Generation rate vs. photon energy and junction depth (x) under monochromatic illumination

Figure 6-c shows in three-dimensional representation the profile of the generation rate versus the radiation energy and the junction depth. The generation rate presents three peaks modeling the absorption of photons by ZnO layer (peak G_{ZnO}), CdS layer (peak G_{CdS}) and $CuInSe_2$ layer (base and region 2 of space charge region) (peak G_{CuInSe_2}). However, the absorption of photons by $CuInS_2$ layer (substrate : x> 1.5 µm) is not visible on the graphs because photons are absorbed by the base ($CuInSe_2$ layer) and do not reach the substrate. The energy band gap of $CuInSe_2$ layer is smaller than the energy band gap of $CuInSe_2$ layer.

Minority carrier densities

Figure 7-a describes the profile of hole density in ZnO layer and CdS layer. The hole density is zero in the non absorption range of ZnO and CdS layers (E ≤2.5 eV). For an absorption of these regions, we note losses of carries at the ZnO surface (part $H_{ZnO(1)}$). The losses of carriers at the ZnO surface and at the ZnO-CdS interface reduce the density of holes in CdS layer and explains the decrease of the global efficiency in the absorption range of these regions.

Figure 7-b shows the electron density profile versus thicknesses in $CuInSe_2$ layer (part H_{CuInSe_2}) and $CuInS_2$ layer (part H_{CuInS_2}). There is no electron density in $CuInS_2$ layer (x> 1.5 µm : part H_{CuInS_2}) for the different illuminations (1.1 eV < E <3.1 eV); there is no generation of carriers in this area, the photons are all absorbed by the base ($CuInSe_2$ layer) placed before the substrate ($CuInS_2$ layer).

In $CuInSe_2$ layer (part H_{CuInSe_2}), the electron density increases when radiation energy decreases, so low energy photons are absorbed in volume with the junction depth. For photons having an energy belonging to the range 1.1 eV <E <1.55 eV largely absorbed by the base, the electron density increases with the thickness of the base and models the diffusion of carriers only towards the space charge region where they will be collected. This diffusion of the electrons only towards the space charge region means that there are not many losses of carriers by recombination at the base-substrate interface. There is no a spike effect at this interface and the low potential barrier between the base and the substrate allows to confine the carriers in the base. The recombination velocity at the base-substrate interface is assumed to be low and fixed at $S_{n_{CuInSe_2/CuInS_2}} = 2 \times 10^3$ cm.s^{-1}.

ISSN: 2277-9655
Impact Factor: 5.164
CODEN: IJESS7

- Three-dimensional modeling of minority carrier densities

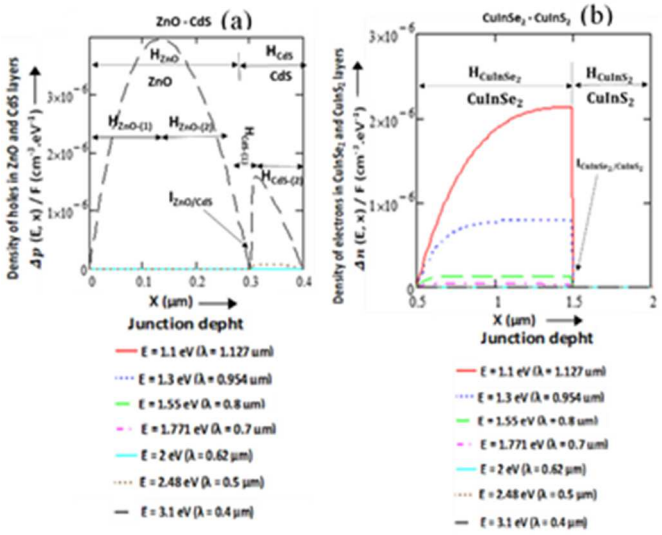

Figure 7. Density of minority carriers photocreated vs. junction depth (x) under monochromatic illumination: a) density of holes in regions 1 and 2 (ZnO-CdS) ; b) density of electrons in regions 3 and 4 (base and substrate : $CuInSe_2$ – $CuInS_2$)

A three-dimensional representation of the minority carrier densities is illustrated on Figures 8-a and 8-b.

Figure 8-a shows the profile of the hole density in ZnO layer (region 1: part H_{ZnO}) and CdS layer (region 2 : part H_{CdS}) versus thickness and energy of incident photons. The cavity observed around 3.3 eV (peak c) shows high losses of carriers in ZnO layer. This figure summarizes in three dimensions the figure 7-a.

Figure 8-b shows the electron density in the rear area ($CuInSe_2$ and $CuInS_2$ layers : base and substrate) versus thickness and energy of incident photons. The part H_{CuInSe_2} represents the profile of the electron density in $CuInSe_2$ layer (base). The part H_{CuInS_2} where the electron density is zero represents the $CuInS_2$ layer (substrate). This figure summarizes in three-dimensional representation the figure 7-b.

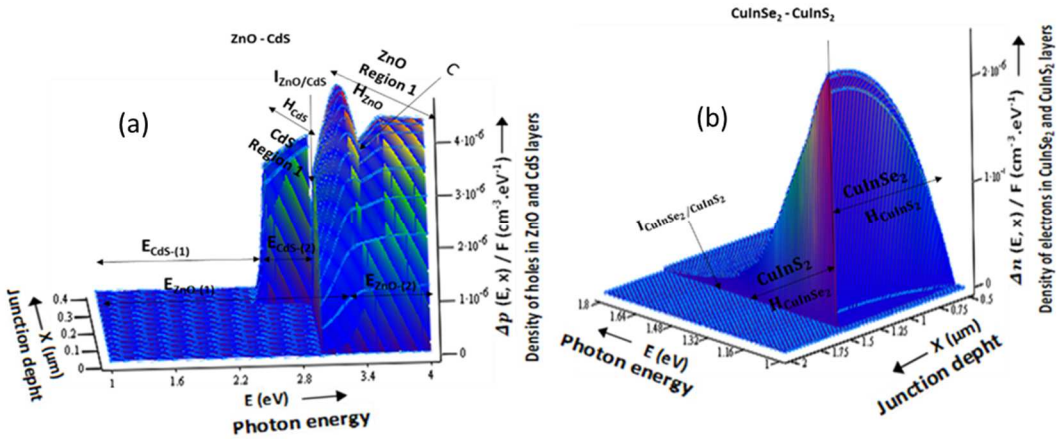

Figure 8. Three-dimensional representation of minority carrier density vs. photon energy and junction depth (x) under monochromatic illumination : (a) hole density in ZnO and CdS layers , (b) electron density in $CuInSe_2$ and $CuInS_2$ layers

3-1-3. photocurrent densities of minority carriers

Figure 9-a shows the hole photocurrent density versus thickness in ZnO layer (parts $H_{ZnO-(1)}$ and $H_{ZnO-(2)}$) and CdS layer (part H_{CdS}) for different radiation energies. The negative part in the ZnO layer (part $H_{ZnO-(1)}$) shows the photocurrent losses on the frontal surface. The presence of the interface is modeled by the discontinuity of the photocurrent for x = 0.3 µm (peak $I_{ZnO/CdS}$).

Figure 9-b shows the hole photocurrent density versus thickness in the space charge region (part W_{CdS} and part W_{CuInSe_2}) For different radiation energies. The photons absorbed by the $CuInSe_2$ layer in the space charge region (part W_{CuInSe_2}) generate a photocurrent of holes which increases simultaneously with the thickness of this region and the energy of radiation. Above 2.5 eV, the front layers (ZnO and CdS) begin to absorb incident photons and

ISSN: 2277-9655
Impact Factor: 5.164
CODEN: IJESS7

reduce the number of photons that reaches the space charge region, causing a drop of the photocurrent of holes in this area. For example, for E = 3.1 eV (λ = 0.4 µm), the hole photocurrent decreases widely and remains constant. It means that the photons having energy greater than 3.1 eV do not reach the space charge region and are all absorbed by the front layers (ZnO and CdS) on a thin thickness lower than 0.4 µm.

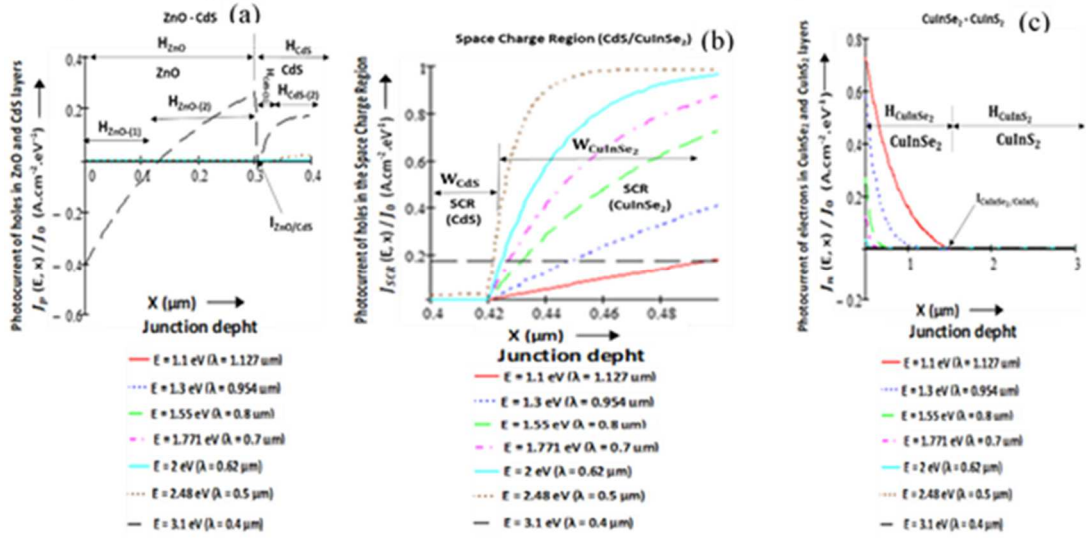

Figure 9. Photocurrent density of minority carriers photocreated vs. junction depth (x) under monochromatic illumination :a) holes in regions 1 and 2 (ZnO-CdS) ; b) holes in the space charge region (CdS/CuInS2) ; c) electrons in regions 3 and 4 (base and substrate : CuInSe2 – CuInS2)

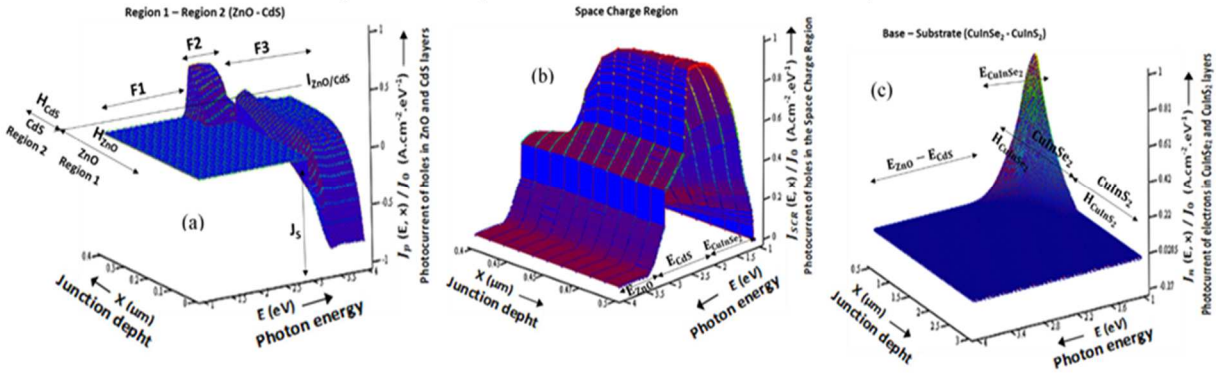

Figure 10. Three-dimensional representation Photocurrent density of minority carriers vs. photon energy and junction depth (x) under monochromatic illumination : a) holes in regions 1 and 2 (ZnO-CdS)) ; b) holes in the space charge region (CdS/ CuInS2) ; c) electrons in regions 3 and 4 (base and substrate : CuInS2 – CuInSe2)

Figure 9-c represents the electron photocurrent density versus the thickness in $CuInSe_2$ layer (base : part H_{CuInSe_2}) and $CuInS_2$ layer (substrate : part H_{CuInS_2}). For each given energy, the electron photocurrent decreases with the thickness of the base and thus models the diffusion of carriers (electrons) only towards the collection area (space charge region) where they will be collected. We also note, in the base (part H_{CuInSe_2}), the photocurrent of electrons increases with decreasing radiation energy because only photons of low energy (1.04 eV <E <1.55 eV) reach the rear area. In the substrate (part H_{CuInS_2}) there is no electron photocurrent density because the photons do not reach this region beyond E = 1.57 eV (energy band gap of $CuInS_2$ layer), they are all absorbed by the base and the space charge region ($CuInSe_2$ layer) on a thin thickness lower than 1 µm. However, we also note that there are no photocurrent losses (no negative electron photocurrent), it means the electrons do not diffuse towards the back surface. Indeed they are blocked by the electrical potential barrier that exists between the base and the substrate, and also the absence of spike effect at the base-substrate interface reduces carrier losses by recombination ($S_{n_{CuInSe_2/CuInS_2}} = 2 \times 10^3$ cm.s^{-1}).

ISSN: 2277-9655
Impact Factor: 5.164
CODEN: IJESS7

- Three-dimensional modeling of photocurrent densities of minority carriers

Figures 10-a, 10-b and 10-c show the evolution of photocurrent of minority carriers versus junction thickness and photon energy (three-dimensional representation) respectively in the front area (ZnO and CdS layers : regions 1 and 2), in the space charge region (CdS / $CuInSe_2$ layers) and in the rear area ($CuInSe_2$ and $CuInS_2$ layers : base and substrate).

Figures 11-a and 11-b respectively represent hole and electron photocurrents versus the thickness of the structure for different radiation energies. The parts R1-R2, SCR-Base, substrate represent the photocurrent of holes (figure 11-a) or electrons (figure 11-b) respectively in regions 1 and 2 (ZnO and CdS layers), in the space charge region (CdS and $CuInSe_2$ layers) and the base ($CuInSe_2$ layer), in the substrate ($CuInS_2$ layer).

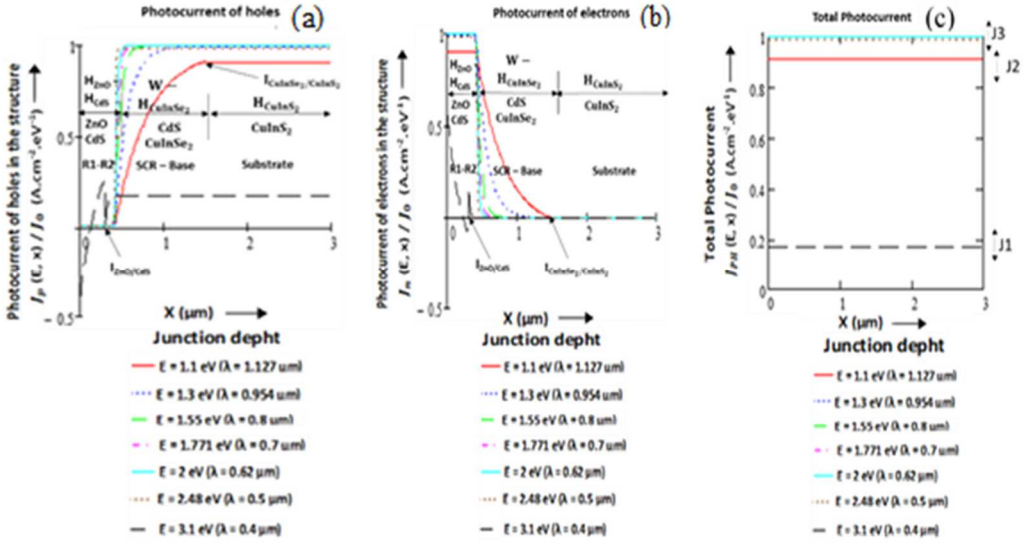

Figure 11. Photocurrent density of minority carriers photocreated vs. junction depth (x) under monochromatic illumination throughout the structure : a) photocurrent density of holes ; b) photocurrent density of electrons , c) total photocourrent

The total photocurrent resulting from the sum of electron photocurrent and hole photocurrent is constant and is shown on Figure 11-c versus thickness of the structure. We note that all carriers generated by photons having energy ranging between 1.3 eV and 2.5 eV, are collected and generate the largest photocurrent (part J3). Photons having low energy ranging between 1.04 eV and 1.3 eV provoke a decrease of the photocurrent (part J2). Indeed they are absorbed in a depth thickness and are not all absorbed by the $CuInSe_2$ layer. The thickness of the $CuInSe_2$ layer is fixed at 1.08 µm located between the space charge region and the base (0.42 µm <x <1.5 µm). Above 3 eV, the absorption of photons by frontal layers (ZnO and CdS layers) strongly reduces the photocurrent (part J1) due to the losses of carriers by recombination phenomenon observed at the ZnO surface and at the ZnO / CdS interface.

Polychromatic illumination under solar spectra AM0, AM1, AM1.5

Generation rate profile under AM0, AM1, AM1.5 solar spectra

On figure 12 we represent three solar spectra of reference versus photon energy [1, 19], allowing to evaluate the theoretical short-circuit photocurrent.

On Figure 13-a, we represent the profile of the generation rate versus junction thickness of the structure for a polychromatic illumination (AM0, AM1 and AM1.5 spectra). The generation rate shows two peaks. A low peak is observed between x = 0.3 µm and x = 0.42 µm (peak G_{CdS}) modeling a weak absorption of photons by the CdS layer. A second peak more elevated is observed between x = 0.42 µm and x = 0.8 µm (peak $G_{CuInSe2}$), it models the absorption of photons by CuInSe2 layer. The low absorption of photons by the CdS layer is due to the low flux of incident photons above 2.5 eV for the different solar spectra (AM0, AM1 and AM1.5). ZnO and $CuInS_2$

ISSN: 2277-9655
Impact Factor: 5.164
CODEN: IJESS7

absorptions are not visible on the graph. For ZnO layer, it absorbs photons above 3.1 eV and in this energy range (E> 3.1 eV) the flux of incident photons is too weak for the different solar spectra (see Figure 12). For the

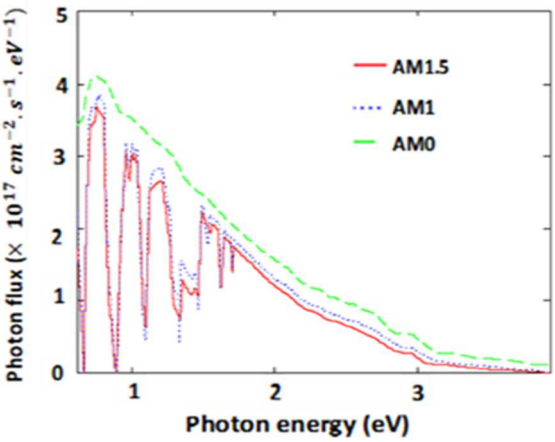

Figure 12. Photon flux vs. photon energy [1, 19]

-absorption of $CuInS_2$ the photons do not reach the substrate, they are all absorbed by the front layers above 1.57 eV ($CuInS_2$ energy band gap). Figure 13-b represents the resulting photocurrent density versus photon energy for the different solar spectra. The short-circuit photocurrent noted Jsc is shown on Figure 13-c for the different solar spectra (AM0, AM1, AM1.5). It is calculated by using a numerical integration method. For this calculation, we use the Newton quadrature. we note:

$$J_{sc} = \int_1^3 J_{ph}(E)dE \approx \frac{\delta E}{2}\left[J_{ph}(E_1) + J_{ph}(E_{m+1}) + 2\sum_{i=2}^{m} J_{ph}(E_i)\right] \quad (39)$$

With: $E \in [1\,,3]\,;\ E_1 = 1\,;\ E_{m+1} = 3\,;\ \delta E = \frac{E_{m+1} - E_1}{m}$

$E_{i+1} = E_1 + i \cdot \delta E$ avec : $i : 1 \ldots m$

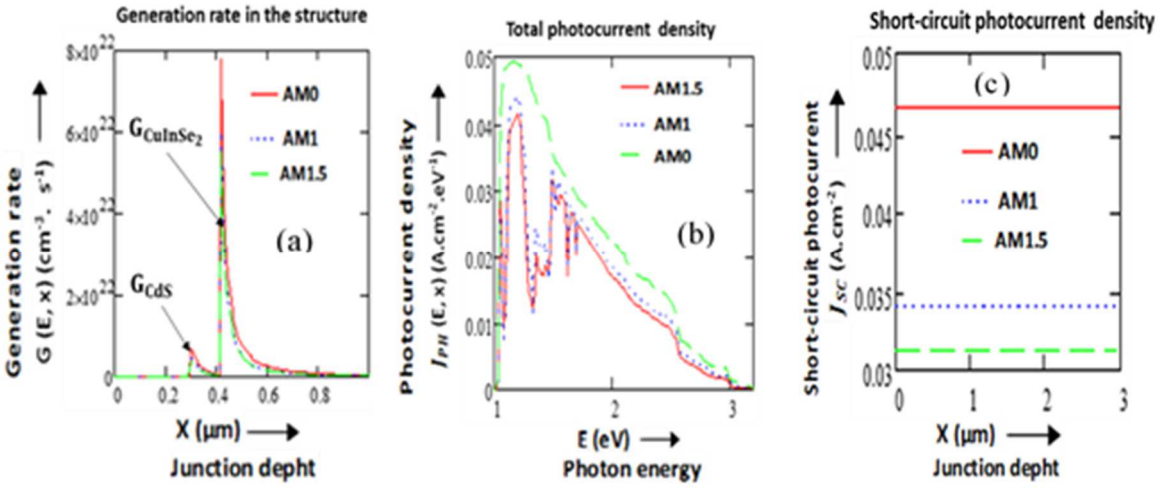

Figure 13. Under polychromatic illumination (AM0, AM1, AM1.5 solar spectra) : (a) Generation rate vs. junction depth (x), (b) total photocurrent density vs. photon energy, (c) short-circuit photocurrent density vs. junction depth (x)

For this calculation, we pose m = 100 and obtain theoretical short-circuit photocurrents represented on figure 13-c and established in table 2 :

Table 2. Theoretical short-circuit photocurrents

AM 0	AM 1	AM 1,5
47 mA.cm^{-2}	34 mA.cm^{-2}	31 mA.cm^{-2}

A relation similar to the expression (39) allows to obtain, the graphs of the generation rate, of the densities of minority carriers and the densities of photocurrent versus junction depth under AM0, AM1 and AM1.5 solar spectra. We always maintain the values used in Table 1.

Minority carrier density and resulting photocurrent profiles under AM0, AM1, AM1.5 solar spectra

Figure 14-a shows the hole density in ZnO (part H_{ZnO}) and CdS (part H_{CdS}) layers and Figure 15-a shows the resulting hole photocurrent in the same regions.

ISSN: 2277-9655
Impact Factor: 5.164
CODEN: IJESS7

Figure 14-b shows the density of electrons versus thickness of the rear area (base and substrate) for a polychromatic illumination (AM0, AM1 and AM1.5 solar spectra). As noted in the case of monochromatic illuminations, in the base (part $H_{CuInSe2}$), the electron density decreases towards the space charge region (0.4 µm≤x≤0.5 µm) where they diffuse before being collected. The increase of electron density towards the base-substrate interface (x = 1.5 µm) is due to the low recombination velocity assumed at the interface ($S_{n_3} = 2 \times 10^3$ cm.s^{-1}) and the confinement of electrons in the base due to the low potential barrier between the base and the substrate. There is no electron density in the substrate (part H_{CuInS2}) because incident photons do not reach this region (see generation rate profile). Figure 15-b shows the photocurrent of electrons in the base and the substrate. In the base (part $H_{CuInSe2}$), as also noted in the case of monochromatic illuminations, the electron photocurrent increases near the space charge region. This increase results from the electron diffusion only towards this collection area. In the substrate (part H_{CuInS2}) there is no electron photocurrent because all photons are absorbed by the frontal layers.

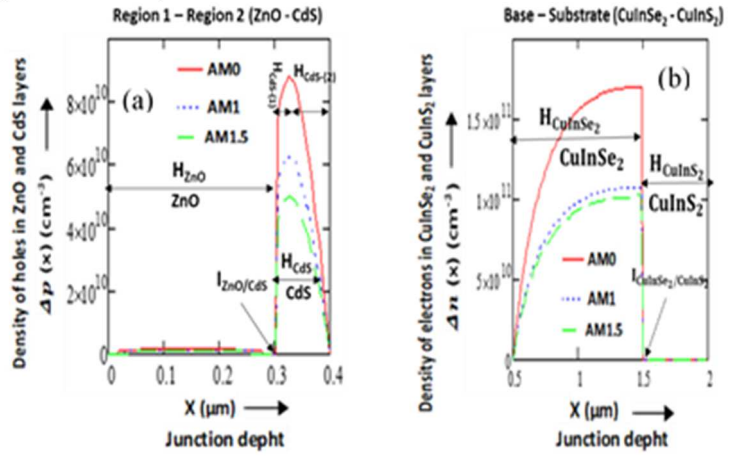

Figure 14. Density of minority carriers photocreated vs. junction depth (x) under polychromatic illumination (AM0, AM1, AM1.5 solar spectra) : a) density of holes in regions 1 and 2 (ZnO-CdS) ; b) density of electrons in regions 3 and 4 (base and substrate : $CuInS_2$ – $CuInSe_2$)

Figure 15-c shows the photocurrent of holes in the space charge region, this photocurrent is quasi-constant in part W_{CdS} which indicates that photons absorbed by the CdS layer do not reach the space charge region , the CdS layer absorbs practically all of them in region 2. The part $W_{CuInSe2}$ models the absorption of photons by the $CuInSe_2$ layer wich causes an increase of the photocurrent with the thickness. Figures 16-a and 16-b represent respectively the hole and electron photocurrents through the different regions of the structure for the different solar spectra (AM0, AM1 and AM1.5).

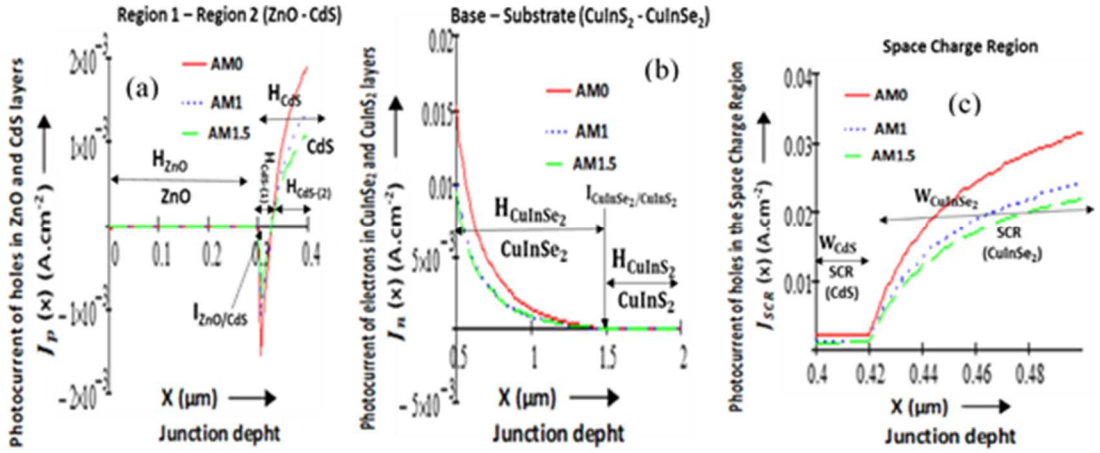

Figure 15. Photocurrent density of minority carriers photocreated vs. junction depth (x) under polychromatic illumination (AM0, AM1, AM1.5 solar spectra) :a) photocurrent density of holes in regions 1 and 2 (ZnO-CdS) ; b) photocurrent density of electrons in regions 3 and 4 (base and substrate : $CuInS_2$ – $CuInSe_2$) ; c) photocurrent density of holes in the space charge region (CdS/ $CuInS_2$)

ISSN: 2277-9655
Impact Factor: 5.164
CODEN: IJESS7

On Figure 16-c, we represent the electron and hole photocurrents and the short-circuit photocurrent versus the junction depth in the same graph for an AM 1.5 solar spectrum. We show the same representation on Figure 16-d for an AM 0 spectrum.

The parts R1-R2, SCR-Base, Substrate represent respectively the considered photocurrent (of electrons, holes or short-circuit) in regions 1 and 2 (ZnO and CdS), in the space charge region and the base (CdS and CuInSe2), in the substrate (CuInSe2).

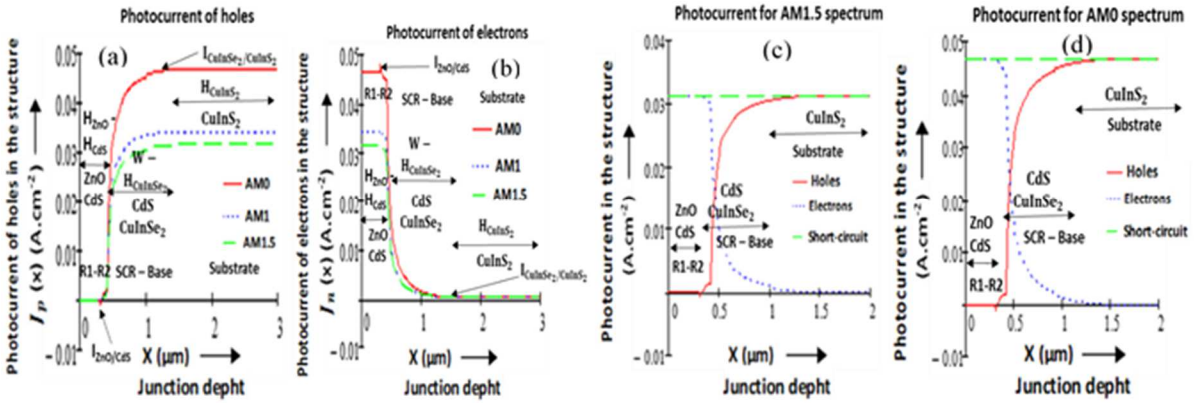

Figure 16. Photocurrent density of minority carriers photocreated vs. junction depth (x) under polychromatic illumination (AM0, AM1, AM1.5 solar spectra) throughout the structure : a) photocurrent density of holes ; b) photocurrent density of electrons; c) electron, hole and short-circuit photocurrents vs. junction depth (x) under polychromatic illumination throughout the structure for AM1.5 solar spectrum ; d) electron, hole and short-circuit photocurrents vs. junction depth (x) under polychromatic illumination throughout the structure for AM0 solar spectrum

4. CONCLUSION

In this work we considered a 4-layer model with a double wide-gap window layer (ZnO and CdS) leading to a $n^+/n/p/p^+$ model of structure. The substrate and the base of the structure are different nature materials and impose boundary conditions that take into account interface effects. For the considered structure ZnO (n +) / CdS (n) / $CuInSe_2$ (p +) / $CuInS_2$ (p), materials are not settled with a decreasing energy band gap. The base ($CuInSe_2$) has the lower energy band gap and a higher photon absorption coefficient, it reacts first and thus reduces substrate contribution. However at the base-substrate interface the energy band diagram constructed according to the Anderson model [20], shows a lack of discontinuity of the valence and conduction bands (no spike effect). This no spike effect, the electrical and lattice parameters fairly close, allow to assume to reduce the recombination rate of the carriers at the base - substrate interface (reduction of the recombination centers). The purpose is to study the behavior of the structure under illumination and optimize performance theoretically.

In this approach, the internal quantum efficiency has been represented and the results obtained show that the spectral response essentially depends on geometrical and electrical parameters (base thickness, diffusion length, recombination rate at the interface, etc.) and their optimization is important for a better performance of the structure.
The studies of the profiles of the generation rate, the minority carrier density and the photocurrent density have been done under monochromatic and polychromatic illumination and shown in three dimensional-representation, to study the intrinsic behavior of the structure originally of the spectral response curves. These studies allow to visualize the behavior of the different areas of the structure, and the effect of the geometrical and electrical parameters on the collection of carriers. Thus, they help to determine the right parameters to enhance the efficiency of the solar cell.

Nomenclature

β : n (electrons) or p (holes) ; i : region (1 : ZnO ; 2 : CdS ; 3 : $CuInSe_2$; 4 : $CuInS_2$)
α_i : Absorption coefficient of region i (cm^{-1})

ISSN: 2277-9655
Impact Factor: 5.164
CODEN: IJESS7

F : Incident photons flux $(cm^{-2}.s^{-1})$
R : Reflection coefficient
τ_{β_i} : Lifetime of free electrons or holes photocreated in region i (μs)
$\Delta\beta_i(x)$: Density of free electrons or holes photocreated in region i at the point of x coordinate (cm^{-3})
$J_{\beta_i}(x)$: Photocurrent density of free electrons or holes photocreated in region i at the point of x coordinate $(A.cm^{-2})$
J_{ph} : Total density of photocurrent $(A.cm^{-2})$
D_{β_i} : Diffusion coefficient of free electrons or holes photocreated in region i $(cm^2.s^{-1})$
L_{β_i} : Diffusion length of free electrons or holes photocreated in region i (μm)
S_{β_i} : Recombination velocity on the surface (or to the interface) of region i $(cm.s^{-1})$
H : Thickness of the structure (μm)
H_i : Thickness of the region i (μm)
w_i : Thickness of the region i of the space charge zone (SCZ) (μm)
q : Elementary charge $(1.6 \times 10^{-19} C)$

REFERENCES

[1] E.M. Keita *, B. Mbow, M.L. Sow , C. Sow , M. Thiam , C. Sene, ''Theoretical Comparative Study Of Internal Quantum Efficiency Of Thin Films Solar Cells Based On CuInSe2 : p+/p/n/n+, p/n/n+, p+/p/n and p/n Models'' International Journal Of Engineering Sciences & Research Technology, 5(9): September, 2016, 344- 359.
[2] C.-H. Huang, ''Effects of Ga content on Cu(In,Ga)Se_2 solar cells studied by numerical modeling'', Journal of Physics and Chemistry of Solids 69 (2008) 330–334.
[3] O. Tesson, M. Morsli, A. Bonnet, V. Jousseaume, L. Cattin, G. Massé'',Electrical characterisation of $CuInSe_2$ thin films for solar cells applications'', Optical Materials, 9(1998) 511.
[4] B. Eisener, M. Wagner, D. Wolf, G. Muller, ''Study of the intrinsic defects in solution grown $CuInSe_2$ crystals depending on the path of crystallization'', J. Cryst Growth, 198-199 (1999) 321.
[5] E.M. Keita, B. Mbow, M.S. Mane, M.L. Sow, C. Sow, C. Sene ''Theoretical Study of Spectral Responses of Homojonctions Based on $CuInSe_2$'' Journal of Materials Science & Surface Engineering, Vol. 4 (4), 2016, pp 392-399.
[6] Subba Ramaiah Kodigala,''Cu(In1-xGax)Se_2 based thin solar cells'', 2010, Volume 35, Academic Press, ELSEVIER.Inc, p. 16.
[7] T. Loher, W. Jaegermann, C. Pettenkofer, ''Formation and electronic properties of the CdS/$CuInSe_2$ (011) heterointerface studied by synchrotron-induced photoemission'', J. Appl. Phys. 77 (1995) 731.
[8] H. Hahn, G. Frank, W. Klinger, A.D. Meyer, G. Stroger, ''Übereinigeternäre Chalkogenidemit Chalcopyritestruktur'',Z. Anorg. Aug. Chem. 271 (1953) 153.
[9] M. Robbins, V.G. Lambrecht Jr., ''Preparation and some properties of materials in systems of the type MIMIIIS2 / MIMIIISe2 where MI = Cu, Ag and MIII = Al, Ga, In'', Mater. Res. Bull. 8 (1973) 703.
[10] I.V. Bodnar, B.V. Korzun, A.I. Lukomski, ''Composition Dependence of the Band Gap of $CuInS_{2x}Se_{2(1-x)}$'', Phys. Stat. Solidi (B) 105 (1981) K143.
[11] S.J. Fonash, Solar Cell device Physics, Academic Press, New York, 1981.
[12] H.L. Hwang, C.Y. Sun, C.Y. Leu, C.C. Cheng, C.C. Tu, '' Growth of $CuInS_2$ and its characterization'', Rev. Phys. Appl. 13 (1978) 745.
[13] Hisashi Yoshikawa, Sadao Adachi, ''Optical Constants of ZnO'', Jpn. J.Appl. Phys. Vol 36 (1997) pp. 6237-6243.
[14] El Hadji Mamadou KEITA, Doctoral Thesis, '' Etude théorique de réponses spectrales de cellules solaires à base de $CuInSe_2$: Modèles à 2 couches (p/n et n/p), à 3 couches (p/n/n+, p+/p/n, n/p/p+ et n+/n/p) et à 4 couches (p+/p/n/n+ et n+/n/p/p+) '', Université Cheikh Anta DIOP de Dakar, Sénégal (2017). P.45-47.

ISSN: 2277-9655
Impact Factor: 5.164
CODEN: IJESS7

[15] B. MBOW, A. MEZERREG, N. REZZOUG, and C.LLINARES, ''Calculated and Measured Spectral Responses in Near-Infrared of III-V Photodetectors Based on Ga, In, and Sb'', phys. Stat. Sol. (a) 141, 511 (1994).
[16] H. J. HOVEL and J. M. WOODALL,'' Ga1-xAlxAs - GaAs P-P-N Heterojunction Solar Cells'', J. Electrochem. Soc. 120, 1246 (1973).
[17] H. J. HOVEL and J. M. WOODALL, 10th IEEE Photovoltaic Specialists Conf., Palo Alto (Calif.) 1973 (p.25).
[18] H. J. HOVEL, ''Semiconductors and Semimetals: Solar Cells'', 11,Academic Press, New York, 127 (1975).
[19] Alain Ricaud, ''Photopiles Solaires'', de la physique de la conversion photovoltaïque aux filières, matériaux et procédés. 1997, 1e édition, Presses polytechniques et universitaires romandes, p.40.
[20] R. L. Anderson, ''Germanium-gallium arsenide heterojunctions'', IBM J.Res.Dev.4, 283, 1960.